Published OnlineFirst August 31, 2018; DOI: 10.1158/1078-0432.CCR-18-0776

Clinical Cancer Research

A Five-MicroRNA Signature Predicts Survival and Disease Control of Patients with Head and Neck Cancer Negative for HPV Infection

Julia Hess[1,2], Kristian Unger[1,2], Cornelius Maihoefer[2,3], Lars Schüttrumpf[2,3], Ludmila Wintergerst[1,2], Theresa Heider[1,2], Peter Weber[1,2,4,5], Sebastian Marschner[2,3], Herbert Braselmann[1,2], Daniel Samaga[1,2], Sebastian Kuger[1], Ulrike Pflugradt[2,3], Philipp Baumeister[2,6], Axel Walch[7], Christine Woischke[8], Thomas Kirchner[8,9], Martin Werner[10,11,12], Kristin Werner[10,11,12], Michael Baumann[13], Volker Budach[14,15], Stephanie E. Combs[9,16,17], Jürgen Debus[18,19], Anca-Ligia Grosu[12,20], Mechthild Krause[13,21,22,23], Annett Linge[13,21,22,23,24], Claus Rödel[25,26], Martin Stuschke[27,28], Daniel Zips[29,30], Horst Zitzelsberger[1,2,3], Ute Ganswindt[2,3,31], Michael Henke[12,20], and Claus Belka[2,3,9]

Abstract

Purpose: Human papillomavirus (HPV)–negative head and neck squamous cell carcinoma (HNSCC) is associated with unfavorable prognosis, while independent prognostic markers remain to be defined.

Experimental Design: We retrospectively performed miRNA expression profiling. Patients were operated for locally advanced HPV-negative HNSCC and had received radiochemotherapy in eight different hospitals (DKTK-ROG; $n = 85$). Selection fulfilled comparable demographic, treatment, and follow-up characteristics. Findings were validated in an independent single-center patient sample (LMU-KKG; $n = 77$). A prognostic miRNA signature was developed for freedom from recurrence and tested for other endpoints. Recursive-partitioning analysis was performed on the miRNA signature, tumor and nodal stage, and extracapsular nodal spread. Technical validation used qRT-PCR. An miRNA–mRNA target network was generated and analyzed.

Results: For DKTK-ROG and LMU-KKG patients, the median follow-up was 5.1 and 5.3 years, and the 5-year freedom from recurrence rate was 63.5% and 75.3%, respectively. A five-miRNA signature (hsa-let-7g-3p, hsa-miR-6508-5p, hsa-miR-210-5p, hsa-miR-4306, and hsa-miR-7161-3p) predicted freedom from recurrence in DKTK-ROG [hazard ratio (HR) 4.42; 95% confidence interval (CI), 1.98−9.88, $P < 0.001$], which was confirmed in LMU-KKG (HR 4.24; 95% CI, 1.40−12.81, $P = 0.005$). The signature also predicted overall survival (HR 3.03; 95% CI, 1.50−6.12, $P = 0.001$), recurrence-free survival (HR 3.16; 95% CI, 1.65−6.04, $P < 0.001$), and disease-specific survival (HR 5.12; 95% CI, 1.88−13.92, $P < 0.001$), all confirmed in LMU-KKG data. Adjustment for relevant covariates maintained the miRNA signature predicting all endpoints. Recursive-partitioning analysis of both samples combined classified patients into low ($n = 17$), low-intermediate ($n = 80$), high-intermediate ($n = 48$), or high risk ($n = 17$) for recurrence ($P < 0.001$).

Conclusions: The five-miRNA signature is a strong and independent prognostic factor for disease recurrence and survival of patients with HPV-negative HNSCC.

[1]Research Unit Radiation Cytogenetics, Helmholtz Zentrum München, German Research Center for Environmental Health GmbH, Neuherberg, Germany. [2]Clinical Cooperation Group "Personalized Radiotherapy in Head and Neck Cancer," Helmholtz Zentrum München, German Research Center for Environmental Health GmbH, Neuherberg, Germany. [3]Department of Radiation Oncology, University Hospital, LMU Munich, Munich, Germany. [4]Institute for Diabetes and Cancer (IDC), Helmholtz Zentrum München, German Research Center for Environmental Health GmbH, Neuherberg, Germany. [5]Joint Heidelberg-IDC Translational Diabetes Program, Heidelberg University Hospital, Heidelberg, Germany. [6]Department of Otorhinolaryngology, Head and Neck Surgery, University Hospital, Ludwig-Maximilians-University of Munich, Munich, Germany. [7]Research Unit Analytical Pathology, Helmholtz Zentrum München, German Research Center for Environmental Health GmbH, Neuherberg, Germany. [8]Institute of Pathology, Faculty of Medicine, Ludwig-Maximilians-University of Munich, Munich, Germany. [9]German Cancer Consortium (DKTK), Partner Site Munich, and German Cancer Research Center (DKFZ), Heidelberg, Germany. [10]Institute for Surgical Pathology, Medical Center-University of Freiburg, Freiburg, Germany. [11]Faculty of Medicine, University of Freiburg, Freiburg, Germany. [12]German Cancer Consortium (DKTK), Partner Site Freiburg, and German Cancer Research Center (DKFZ), Heidelberg, Germany. [13]German Cancer Consortium (DKTK), Partner Site Dresden, and German Cancer Research Center (DKFZ), Heidelberg, Germany. [14]Department of Radiooncology and Radiotherapy, Charité University Hospital Berlin, Berlin, Germany. [15]German Cancer Consortium (DKTK), Partner Site Berlin, and German Cancer Research Center (DKFZ), Heidelberg, Germany. [16]Department of Radiation Oncology, Klinikum rechts der Isar, Technische Universität München, Munich, Germany. [17]Institute of Innovative Radiotherapy (iRT), Helmholtz Zentrum München, German Research Center for Environmental Health GmbH, Neuherberg, Germany. [18]Department of Radiation Oncology, Heidelberg Ion Therapy Center (HIT), University of Heidelberg, Heidelberg, Germany. [19]German Cancer Consortium (DKTK), Partner Site Heidelberg, and German Cancer Research Center (DKFZ), Heidelberg, Germany. [20]Department of Radiation Oncology, Medical Center, Faculty of Medicine, University of Freiburg, Freiburg, Germany. [21]Department of Radiotherapy and Radiation Oncology, Faculty of Medicine and University Hospital Carl Gustav Carus, Technische Universität Dresden, Dresden, Germany. [22]OncoRay – National Center for

Published OnlineFirst August 31, 2018; DOI: 10.1158/1078-0432.CCR-18-0776

Translational Relevance

Human papillomavirus (HPV)–negative head and neck squamous cell carcinoma (HNSCC) is currently treated with a set of standard-of-care therapeutic approaches that in total result in approximately 50% overall survival for locally advanced HNSCC, demonstrating that substantial subgroups are not likely to profit from state-of-the-art therapy. The most relevant clinical event limiting success of HNSCC therapy is recurrence of the disease after surgical tumor resection followed by radio(chemo)therapeutic treatment. The presented HNSCC HPV-negative five-miRNA signature predicts the risk for recurrence in HNSCC and allows, in combination with the clinically established risk factors, the definition of four prognostically distinct groups. This provides the first prerequisite for the consideration of personalized treatment approaches in HPV-negative HNSCC. Possible personalized treatment options include consideration of adjusting therapy intensity according to the overall risk for therapy failure in the first line. Further, and most importantly, it represents the basis for a more focused search for molecular therapeutic targets, improving therapy success for appropriate patients.

Introduction

Prognosis of patients with locally advanced head and neck squamous cell carcinoma (HNSCC) generally remains poor. Whereas patients with high-risk human papillomavirus (HPV) associated HNSCC have a considerably more favorable outcome, HPV-negative patients still have to expect limited disease control and survival (1, 2). From the biologic perspective, intrinsic resistance of tumor cells to radiochemotherapy or therapy failure caused by metastatic spread are possible underlying factors. Consequently, research aims at altering radiation dose and fractionation or—more recently—at the additional administration of targeted drugs and/or immune-checkpoint inhibitors (3, 4). However, biomarkers to predict which patients potentially would profit from these approaches are missing.

Complex and heterogeneous genomic aberrations and mutation patterns molecularly control initiation and progression of HNSCC (5–7). MicroRNAs (miRNA), involved in posttranscriptional regulation, have been shown to be highly deregulated in most cancers and might well be of prognostic relevance (8, 9). In HNSCC, aberrantly expressed miRNAs were described (10–12). However, so far no study has investigated the prognostic role of miRNAs by comprehensive miRNA profiling in well-characterized HPV-negative HNSCC cohorts.

Here, we analyzed miRNA expression profiles in cancer tissue of locally advanced HNSCC ($n = 162$). We hypothesized that we can develop an miRNA-based molecular signature, which allows to stratify HPV-negative HNSCC patients according to risk of recurrence following adjuvant radio(chemo)therapy.

Materials and Methods

Patient specimens and study design

In the present study, we analyzed two independent samples of HNSCC patients who had undergone surgical resection followed by adjuvant radio(chemo)therapy: the DKTK-ROG (German Consortium for Translational Cancer Research, Radiation Oncology Group) and the LMU-KKG (Ludwig-Maximilians-University of Munich, Clinical Cooperation Group "Personalized Radiotherapy in Head and Neck Cancer") samples. For both samples, clinical data and treatment-naïve patient tissue specimens were collected retrospectively. All patients were diagnosed with histologically proven HNSCC of the hypopharynx, oropharynx, or the oral cavity. Only HPV-negative HNSCC were included (Supplementary Methods). Ethical approval (EA) for this retrospective study, carried out in accordance with the Declaration of Helsinki, was obtained by the ethics committees of all DKTK-ROG partners including the LMU (EA 312-12, 448-13, 17-116). Tumor stage was assessed using the Union for International Cancer Control Tumor–Node–Metastasis (UICC TNM) Classification of Malignant Tumors, 7th edition.

The multicentric study sample DKTK-ROG originally included 221 HNSCC patients treated at one of the eight different DKTK partner sites (13). This study reports on 85 of 143 patients with HPV-negative tumors who were treated between 2005 and 2011. Fifty-eight patients had to be omitted due to insufficient tumor material. All patients received postoperative radiotherapy covering the previous tumor region and regional lymph nodes with concurrent cisplatin (CDDP)-based chemotherapy according to standard protocols. Inclusion criteria were positive microscopic resection margins and/or extracapsular extension (ECE) of lymph nodes and/or tumor stage pT4 and/or more than three positive lymph nodes. The median overall treatment time was 44 days [interquartile range (IQR),

Radiation Research in Oncology, Faculty of Medicine and University Hospital Carl Gustav Carus, Technische Universität Dresden, Dresden, Germany. [23]National Center for Tumor Diseases (NCT), Partner Site Dresden, Dresden, Germany. [24]Helmholtz-Zentrum Dresden – Rossendorf, Institute of Radiooncology – OncoRay Dresden, Dresden, Germany. [25]Department of Radiotherapy and Oncology, Goethe-University Frankfurt, Frankfurt, Germany. [26]German Cancer Consortium (DKTK), Partner Site Frankfurt, and German Cancer Research Center (DKFZ), Heidelberg, Germany. [27]Department of Radiotherapy, Medical Faculty, University of Duisburg-Essen, Essen, Germany. [28]German Cancer Consortium (DKTK), Partner Site Essen, and German Cancer Research Center (DKFZ), Heidelberg, Germany. [29]Department of Radiation Oncology, Faculty of Medicine and University Hospital Tübingen, Eberhard Karls University Tübingen, Tübingen, Germany. [30]German Cancer Consortium (DKTK), Partner Site Tübingen, and German Cancer Research Center (DKFZ), Heidelberg, Germany. [31]Department of Therapeutic Radiology and Oncology, Innsbruck Medical University, Innsbruck, Austria.

Note: Supplementary data for this article are available at Clinical Cancer Research Online (http://clincancerres.aacrjournals.org/).

J. Hess and K. Unger contributed equally to this article and share first authorship.

M. Henke and C. Belka contributed equally to this article and share senior authorship.

Corresponding Author: Julia Hess, Helmholtz Zentrum München, German Research Center for Environmental Health GmbH, Ingolstädter Landstrasse 1, 85764 Neuherberg, Germany. Phone: 49-89-3187-3517; Fax: 49-89-3187-2146; E-mail: julia.hess@helmholtz-muenchen.de

doi: 10.1158/1078-0432.CCR-18-0776

43–46 days]. Adjuvant radiotherapy including elective irradiation of cervical lymph nodes was applied with a median dose of 50 Gy (median dose 2 Gy/fraction) and a boost to the former tumor region and to microscopic disease (if any) to a median dose of 66 Gy (median dose 2 Gy/fraction). Cisplatin was applied weekly with a median cumulative dose of 200 mg/m^2 body surface area (BSA; range, 100–300 mg/m^2 BSA).

The monocentric study sample LMU-KKG included originally all HNSCC patients with at least UICC TNM stage III or close/positive microscopic resection margins (resection margins were considered "close margin" when declared R0, but less than 5 mm by the local pathologist) who were treated with adjuvant radiotherapy between June 2008 and January 2013 at the LMU Department of Radiation Oncology (14). The median overall treatment time was 45 days (IQR, 43–47 days) with five fractions per week. A median radiation dose of 64 Gy (median dose 2 Gy/fraction) was applied to the former tumor bed or regions of ECE, elective lymph node regions have been covered according to tumor stage and localization with a median dose of 50 Gy (median dose 2 Gy/fraction) and 56 Gy (median dose 2 Gy/fraction) was applied to involved lymph node regions.

In the case of close/positive microscopic resection margins and/or ECE, patients received concurrent chemotherapy. The majority (76%) of the patients received CDDP/5-fluorouracil (5-FU; CDDP: 20 mg/m^2 BSA days 1–5/29–33; 5-FU: 600 mg/m^2 BSA days 1–5/29–33). In selected cases, Mitomycin C (MMC) or 5-FU/MMC replaced platin-based chemotherapy. This study reports on the HPV-negative tumor subset ($n = 77$) of all patients with available tumor tissue specimens ($n = 115$).

After histopathologic review of hematoxylin and eosin–stained tissue sections from available blocks with formalin-fixed and paraffin-embedded (FFPE) tumor tissue by a pathologist (DKTK-ROG: K. Werner; LMU-KKG: C. Woischke/A. Walch), the tumor area was annotated. If necessary, microdissection was performed prior nucleic acids extraction in order to ensure a tumor cellularity (i.e., the percentage of tumor cells in analyzed tissue) of at least 60% (DKTK-ROG: median 60%, IQR, 60%–70%; LMU-KKG: median 70%, IQR, 70%–80%).

Procedures

Total RNA, including the small RNA fraction, was extracted using the Qiagen miRNeasy FFPE (DKTK-ROG) or the AllPrep DNA/RNA FFPE Kit (LMU-KKG) according to the manufacturer's protocols (Qiagen). Isolated RNA was quantified with the Qubit-Fluorometer and integrity of small RNAs was assessed (Supplementary Methods).

miRNA expression was profiled using SurePrint G3 8 × 60K Human miRNA Microarrays (AMADID 70156; Agilent Technologies) representing 2,549 human miRNAs (content sourced from miRBase database, Release 21.0; Supplementary Methods). Microarray raw data were uploaded to the publicly available database ArrayExpress (accession no. E-MTAB-5793). miRNA expression microarray profiling resulted in a data set of 162 HNSCC samples (DKTK-ROG: $n = 85$; LMU-KKG: $n = 77$).

Data analysis was performed using the R statistical software (version 3.3.1) in combination with R-Bioconductor/CRAN packages (Supplementary Methods; ref. 15).

For the purpose of building a Cox proportional hazards model predicting disease recurrence in combination with miRNA expression, we used a robust likelihood-based survival modeling approach deploying an iterative forward-selection algorithm implemented in the R-package rbsurv (16). We recently built an miRNA signature predicting outcome in glioblastoma using the same approach (Supplementary Methods; ref. 17).

Experimentally validated miRNA-target genes of the signature miRNAs were obtained from the miRTarBase database (Release 6.0). The Cytoscape software (version 3.2.1) with the Reactome FI plugin (version 4.0.0) was used to generate an miRNA–mRNA target regulatory network and to conduct pathway enrichment analysis of the target genes. Pathways with $P < 0.05$ were considered as significantly enriched with target genes (18).

For technical validation of microarray data, qRT-PCR analysis was performed (Supplementary Methods).

Clinical endpoints and statistical analysis

As the main objective of the study was the identification of an miRNA signature that allows separation of patients according to risk of recurrence, the primary endpoint was freedom from recurrence. Freedom from recurrence was defined as the time (days) from the start of radiotherapy treatment to the time of the first observation of confirmed locoregional or distant recurrence. Data for recurrence-free patients were right censored either at the date of death or last follow-up visit. Additional endpoints included were recurrence-free survival, overall survival, disease-specific survival, disease-unspecific survival, distant control, and locoregional control. We calculated recurrence-free survival (days) from the date of radiotherapy treatment start to the first observation of locoregional/distant recurrence or death due to any cause; overall survival from the date of radiotherapy treatment start to the date of death from any cause; disease-specific survival from the date of radiotherapy treatment start to the date of tumor related death; non–tumor-related survival from the date of radiotherapy treatment start to the date of non–tumor-related death; distant control from the date of radiotherapy treatment start to the date of distant recurrence; and locoregional control from the date of radiotherapy treatment start to the date of local recurrence. In the absence of an event, patients were censored at the date of the last follow-up visit (or the date of death).

Kaplan–Meier curves were compared for statistical difference using the log-rank test using the R-package survival. Median time-to-event estimates and hazard ratios (HR) with 95% confidence intervals (CI) were determined. Univariate Cox proportional hazard analysis was performed to evaluate the association of clinicopathologic variables with outcome (Supplementary Methods). We used multivariate Cox proportional hazards analysis to assess the prognostic value of the identified miRNA signature after adjustment for other prognostic clinical parameters as covariates.

The clinical endpoint prediction performance of the five-miRNA signature and clinicopathologic variables in terms of sensitivity and specificity, represented by the corresponding areas under the curve (AUC), was determined for follow-up times from 1 to 5 years (Supplementary Methods).

Recursive-partitioning analysis (RPA) for the generation of a decision tree considering the clinical parameters ECE status, TNM T stage, TNM N stage, and resection margin status with or without the five-miRNA signature defined risk

Published OnlineFirst August 31, 2018; DOI: 10.1158/1078-0432.CCR-18-0776

groups was conducted using the R-package rpart (Supplementary Methods).

Results

The clinicopathologic characteristics of the HNSCC patients included in our study (median follow-up: DKTK-ROG 5.1 years, IQR 3.7–5.6; LMU-KKG 5.3 years, IQR 4.4–6.4) are listed in Table 1. Compared with the DKTK-ROG sample, which exclusively contained patients treated by postoperative radiotherapy with concurrent cisplatin-based chemotherapy, only 63.6% of the LMU-KKG sample received concurrent radiochemotherapy. Accordingly, the LMU-KKG sample contained fewer patients with UICC TNM stage IV, advanced nodal stage, ECE or positive microscopic resection margins. Of all patients, 31.5% (51/162) developed disease recurrence within the observed follow-up time while the two samples did not differ with regard to the endpoints freedom from recurrence and recurrence-free survival (Supplementary Fig. S1). The 5-year freedom from recurrence rate was 63.5% and 75.3% for DKTK-ROG and LMU-KKG patients, respectively.

The miRNA expression profiling of 162 tumor specimens identified 1,031 expressed miRNAs. After univariate preselection 524 miRNAs remained for feature selection using a robust likelihood-based survival modeling forward-selection approach (Supplementary Table S1). The best model according to the Akaike information criterion contained the five miRNAs—hsa-let-7g-3p, hsa-miR-6508-5p, hsa-miR-210-5p, hsa-miR-4306, and hsa-miR-7161-3p—with the following Cox proportional hazard coefficients: −0.5214183, −0.5254865, 0.6461524, −0.3678727, and −0.8165854, respectively. The coefficients were subsequently used for individual risk score calculation after linear combination with appropriate expressions of the signature miRNAs. Using the median risk score as a cutoff, 43 patients of the DKTK-ROG sample (training set) were assigned to the low-risk group [median time to event not reached (NR); 95% CI, 2047−not estimable (NE); eight events] and 42 to the high-risk group (median time to event 748 days; 95% CI, 459–NE; 24 events). As expected, the groups differed significantly in their risk of recurrence (HR 4.42; 95% CI, 1.98−9.88; log-rank $P < 0.001$; Fig. 1A; Supplementary Fig. S2).

We applied the five-miRNA–based signature prediction model to the miRNA expression data set of the LMU-KKG sample (validation set) using the cutoff as calculated from the training sample data (0.03629712) and assigned 38 patients to the low-risk (median NR; 95% CI, NE−NE; four events) and 39 patients to the high-risk group (median NR; 95% CI, 708−NE; 15 events). The risk for recurrence of the high-risk patients was significantly increased compared with that of the low-risk patients (HR 4.24; 95% CI, 1.40−12.81; $P = 0.005$), confirming the prognostic value of the five-miRNA signature (Fig. 1A; Supplementary Fig. S2). miRNA-based risk group classification was not associated with simultaneous chemotherapy treatment (Table 1), which was further supported after stratification to LMU-KKG patients treated by concurrent radiochemotherapy ($n = 49$; HR 3.85; 95% CI, 1.09–13.58, $P = 0.024$; Supplementary Fig. S3).

Moreover, high-risk patients of both samples showed significantly reduced recurrence-free survival, overall survival, and disease-specific survival rates (Fig. 1B). We could also demonstrate an impact of both failure sites (locoregional and distant) on the risk stratification, while low- and high-risk patients did not differ in non–tumor-related death (Supplementary Fig. S4).

In order to assess whether the five-miRNA signature was an independent prognosticator, associations of known clinicopathologic factors with the miRNA-defined risk groups were tested. TNM T stage, ECE, and tumor localization were associated with the miRNA risk groups (Table 1). In the subsequent univariate Cox proportional hazard analysis, TNM T stage and lymphovascular invasion (LVI) were significantly associated with freedom from recurrence in both samples, ECE was identified as a significant parameter in the DKTK-ROG sample only, whereas no differences between the three tumor localizations were observed (Supplementary Table S2; Supplementary Figs. S5–S7). After adjustment for these parameters in multivariate Cox regression analysis, the five-miRNA signature retained its independent and exclusive prognostic role in both samples (training set: HR 5.55; 95% CI, 2.09–14.79, $P < 0.001$; validation set: HR 3.94; 95% CI, 1.23–12.59, $P = 0.021$; Table 2).

We analyzed the sensitivity and specificity of the five-miRNA signature in the prediction of different clinical endpoints in comparison with the clinical prognostic parameters TNM T stage, LVI, and ECE. At 5 years follow-up, the five-miRNA signature demonstrated a superior prediction of all endpoints analyzed (Fig. 2A; Supplementary Fig. S8). Furthermore, in time-dependent analysis (follow-up years 1–5), the five-miRNA signature superiorly predicted all endpoints from 2 to 5 years compared with the clinicopathologic parameters. After 1-year follow-up, higher AUCs for the miRNA signature compared with the analyzed endpoints were observed only in the training set for the endpoints disease-specific survival and overall survival (Figs. 2B; Supplementary Figs. S9 and S10). After combining the five-miRNA signature with the clinicopathologic parameters (TNM T stage, LVI, and ECE) an even better prediction of all endpoints from 2 to 5 years was achieved for both HNSCC samples, also when compared with combinations of the clinicopathologic risk factors (Fig. 2C; Supplementary Fig. S11). This was also the case after 1-year follow-up in the DKTK-ROG sample.

In order to obtain deeper insights into the biological regulatory function of the signature miRNAs, we generated an miRNA–mRNA target regulatory network comprising experimentally validated miRNA-target interactions, whereby 12 target genes were found to be shared by the signature miRNAs (Supplementary Table S3; Supplementary Fig. S12). Pathway enrichment analysis of the target genes revealed 36 pathways including *p53*, *ATM*, and *FoxO* signaling, DNA double-strand break response, pre-NOTCH expression and processing, mitosis, and senescence-associated pathways (Supplementary Table S4).

For technical validation of the five-miRNA signature and potential clinical diagnostic application, we measured the expression of the signature miRNAs in the validation set ($n = 71$) by qRT-PCR confirming the microarray-derived results as the miRNA-classified risk groups significantly differed in freedom of recurrence (HR 5.07; 95% CI, 1.17−21.94, $P = 0.016$; Supplementary Fig. S13).

In a Kaplan–Meier analysis in which the samples were pooled ($n = 162$) and stratified according to resection margin status, TNM T stage, TNM N stage, ECE, and tumor localization, the resulting five-miRNA signature risk groups significantly differed in clinical outcome (Supplementary Figs. S14 and S15). This motivated us to further combine the five-miRNA signature with clinically relevant

Published OnlineFirst August 31, 2018; DOI: 10.1158/1078-0432.CCR-18-0776

Table 1. Clinical and pathologic characteristics of HNSCC patients included in the DKTK-ROG and LMU-KKG samples and stratified according to the five-miRNA signature

	Training set DKTK-ROG ($n = 85$)				Validation set LMU-KKG ($n = 77$)			
	Number of all patients	Low-risk ($n = 43$)	High-risk ($n = 42$)	*P* value[a]	Number of all patients	Low-risk ($n = 38$)	High-risk ($n = 39$)	*P* value[a]
Age (years)				0.77				0.86
<45	7 (8%)	2 (5%)	5 (12%)		3 (4%)	1 (3%)	2 (5%)	
45–54	26 (31%)	13 (30%)	13 (31%)		17 (22%)	7 (18%)	10 (26%)	
55–64	35 (41%)	18 (42%)	17 (40%)		28 (36%)	15 (39%)	13 (33%)	
65–74	17 (20%)	10 (23%)	7 (17%)		26 (34%)	13 (34%)	13 (33%)	
>75	0	0	0		3 (4%)	2 (5%)	1 (3%)	
Sex				1.0				1.0
Male	67 (79%)	34 (79%)	33 (79%)		52 (68%)	26 (68%)	26 (67%)	
Female	18 (21%)	9 (21%)	9 (21%)		25 (32%)	12 (32%)	13 (33%)	
Tumor localization				0.12				0.022
Hypopharynx	13 (15%)	9 (21%)	4 (10%)		15 (19%)	4 (11%)	11 (28%)	
Oral cavity	32 (38%)	12 (28%)	20 (48%)		27 (35%)	11 (29%)	16 (41%)	
Oropharynx	40 (47%)	22 (51%)	18 (43%)		35 (45%)	23 (61%)	12 (31%)	
UICC TNM stage				0.56				0.79
I	0	0	0		2 (3%)	1 (3%)	1 (3%)	
II	3 (4%)	2 (5%)	1 (2%)		6 (8%)	4 (11%)	2 (5%)	
III	13 (15%)	5 (12%)	8 (19%)		23 (30%)	12 (32%)	11 (28%)	
IV	69 (81%)	36 (84%)	33 (79%)		46 (60%)	21 (55%)	25 (64%)	
T stage				0.33				0.042
T1	12 (14%)	9 (21%)	3 (7%)		17 (22%)	9 (24%)	8 (21%)	
T2	35 (41%)	17 (40%)	18 (43%)		29 (38%)	18 (47%)	11 (28%)	
T3	22 (26%)	10 (23%)	12 (29%)		21 (27%)	10 (26%)	11 (28%)	
T4	16 (19%)	7 (16%)	9 (21%)		10 (13%)	1 (3%)	9 (23%)	
N stage				0.14				0.41
N0	10 (12%)	5 (12%)	5 (12%)		19 (25%)	8 (21%)	11 (28%)	
N1	10 (12%)	2 (5%)	8 (19%)		20 (26%)	10 (26%)	10 (26%)	
N2	57 (67%)	33 (77%)	24 (57%)		36 (47%)	20 (53%)	16 (41%)	
N3	8 (9%)	3 (7%)	5 (12%)		2 (3%)	0	2 (5%)	
Lymphovascular invasion (LVI)				0.46				1.0
0	42 (49%)	25 (58%)	17 (40%)		50 (65%)	26 (68%)	24 (62%)	
1	27 (32%)	13 (30%)	14 (33%)		17 (22%)	9 (24%)	8 (21%)	
Missing information	16 (19%)	5 (12%)	11 (26%)		10 (13%)	3 (8%)	7 (18%)	
Venous tumor invasion (VTI)				1.0				1.0
0	62 (73%)	33 (77%)	29 (69%)		66 (86%)	34 (89%)	32 (82%)	
1	7 (8%)	4 (9%)	3 (7%)		3 (4%)	2 (5%)	1 (3%)	
Missing information	16 (19%)	6 (14%)	10 (24%)		8 (10%)	2 (5%)	6 (15%)	
Perineural invasion (PNI)				1.0				0.55
0	0	0	0		37 (48%)	19 (50%)	18 (46%)	
1	0	0	0		15 (19%)	6 (16%)	9 (23%)	
Missing information	85 (100%)	43 (100%)	42 (100%)		25 (32%)	13 (34%)	12 (31%)	
Resection margin status				0.52				0.49
0	45 (53%)	21 (49%)	24 (57%)		57 (74%)	28 (74%)	29 (74%)	
1	40 (47%)	22 (51%)	18 (43%)		17 (22%)	7 (18%)	10 (26%)	
2	0	0	0		1 (1%)	1 (3%)	0	
Missing information	0	0	0		2 (3%)	2 (5%)	0	
ECE				0.007				0.38
Yes	41 (48%)	14 (33%)	27 (64%)		25 (32%)	11 (29%)	14 (36%)	
No	34 (40%)	24 (56%)	10 (24%)		32 (42%)	19 (50%)	13 (33%)	
Not applicable (N0)	10 (12%)	5 (12%)	5 (12%)		19 (25%)	8 (21%)	11 (28%)	
Missing information	0	0	0		1 (1%)	0	1 (3%)	
Grading				0.56				0.29
1 (well differentiated)	3 (4%)	2 (5%)	1 (2%)		2 (3%)	2 (5%)	0	
2 (moderately differentiated)	50 (59%)	23 (53%)	27 (64%)		34 (44%)	15 (39%)	19 (49%)	
3 (poorly differentiated)	32 (38%)	18 (42%)	14 (33%)		41 (53%)	21 (55%)	20 (51%)	
ECOG performance status				0.64				0.20
0	18 (21%)	8 (19%)	10 (24%)		13 (17%)	4 (11%)	9 (23%)	
1	33 (39%)	17 (40%)	16 (38%)		40 (52%)	21 (55%)	19 (49%)	
2	6 (7%)	4 (9%)	2 (5%)		5 (6%)	1 (3%)	4 (10%)	
Missing information	28 (33%)	14 (33%)	14 (33%)		19 (25%)	12 (32%)	7 (18%)	
Smoking status				0.18				0.68
Nonsmoker	5 (6%)	4 (9%)	1 (2%)		6 (8%)	2 (5%)	4 (10%)	
Smoker	52 (61%)	23 (53%)	29 (69%)		52 (68%)	25 (66%)	27 (69%)	
Missing information	28 (33%)	16 (37%)	12 (29%)		19 (25%)	11 (29%)	8 (21%)	

(Continued on the following page)

Published OnlineFirst August 31, 2018; DOI: 10.1158/1078-0432.CCR-18-0776

Table 1. Clinical and pathologic characteristics of HNSCC patients included in the DKTK-ROG and LMU-KKG samples and stratified according to the five-miRNA signature (Cont'd)

	Training set DKTK-ROG ($n = 85$)				Validation set LMU-KKG ($n = 77$)			
	Number of all patients	Low-risk ($n = 43$)	High-risk ($n = 42$)	*P* value[a]	Number of all patients	Low-risk ($n = 38$)	High-risk ($n = 39$)	*P* value[a]
Smoking history—pack-years				0.20				0.67
≤10 (including nonsmokers)	7 (8%)	5 (12%)	2 (5%)		6 (8%)	2 (5%)	4 (10%)	
>10	23 (27%)	9 (21%)	14 (33%)		48 (62%)	25 (66%)	23 (59%)	
Missing information	55 (65%)	29 (67%)	26 (62%)		23 (30%)	11 (29%)	12 (31%)	
Simultaneous chemotherapy				1.0				0.16
Yes	85 (100%)	43 (100%)	42 (100%)		49 (64%)	21 (55%)	28 (72%)	
No	0	0	0		28 (36%)	17 (45%)	11 (28%)	

NOTE: Data are numbers (%).

Abbreviation: ECOG, Eastern Cooperative Oncology Group.

[a]Chi-square test or Fisher exact test.

parameters. RPA identified four different risk groups for recurrence ("low-risk," "low-intermediate-risk," "high-intermediate-risk," and "high-risk"), including the five-miRNA signature as strongest parameter together with TNM T stage, ECE, and TNM N stage (Fig. 3 and extended version Supplementary Fig. S16). The worst prognostic group included miRNA signature high-risk patients with ECE-positive T3/T4 tumors (median freedom from recurrence 438 days), while miRNA signature low-risk patients with T1/T2 N0/N1 HNSCC had the best prognosis (no event). The four risk groups also significantly differed with regard to locoregional and distant control, recurrence-free survival, overall survival and disease-specific survival (Supplementary Figs. S17 and S18). RPA considering only the clinical parameters identified three risk groups for recurrence with T stage as the strongest parameter together with ECE and N stage (Supplementary Fig. S19A). Combining the three RPA-derived risk groups with the risk factor of our five-miRNA signature revealed patient subgroups significantly differing in clinical outcome ("RPA intermediate-risk": HR 2.71; 95% CI, 1.21–6.06, $P = 0.012$; "RPA high-risk": HR 12.20; 95% CI, 1.54–96.90, $P = 0.004$; Supplementary Fig. S19B).

Discussion

Here we report, for the first time, a five-miRNA signature in HPV-negative patients that predicts decreased cancer control following adjuvant radiochemotherapy. Freedom from recurrence was the chosen primary endpoint to better estimate treatment effects, as HNSCC patients often suffer from multiple comorbidities that affect overall survival (19). Overall, baseline and treatment characteristics of our patients were balanced and compare well to reports on HPV-negative HNSCC. Remarkably, our identified five-miRNA signature predicts survival as well. Of note, its prognostic significance is independent from known clinical parameters.

A potential limitation of the study is the fact that clinical data for both samples were obtained retrospectively. We thus cannot fully exclude certain selection bias. Heterogeneity due to inclusion of a multicenter HNSCC patient sample minimized and potentially excluded selection bias. In addition, the signature's robustness and potential clinical applicability was underlined by identification in a multicenter sample and validation in an independent monocentric sample. Most other studies introducing prognostic miRNA signatures (e.g., ovarian, nasopharyngeal, and colon cancer) followed a comparable strategy (8, 20, 21).

The fact that the DKTK-ROG sample exclusively included HNSCC patients treated by postoperative radiochemotherapy, whereas the LMU-KKG sample comprised both adjuvant treatment groups—radiotherapy with simultaneous chemotherapy and radiotherapy alone—might be seen as another limitation of our study. However, from our point of view, the independence of the five-miRNA signature from the addition of simultaneous chemotherapy even strengthens the potential of our five-miRNA signature.

A further potential shortcoming of our study is that the final RPA was limited by small numbers of patients. In order to achieve the highest possible number of cases and the maximum statistical power, we pooled both HNSCC samples for this analysis ($n = 162$). In all clinical endpoints, a significant separation of risk groups defined by clinical risk factors combined with the five-miRNA signature was achieved.

To substantiate our findings on patient stratification into risk groups, further validation of our five-miRNA signature in independent retrospective and in particular prospective patient populations with fully annotated clinical data will be important future steps.

Previous studies have identified multiple deregulated miRNAs in HNSCC partly with prognostic relevance for patients (10–12, 22–26). A meta-analysis revealed that in particular overexpression of miR-21, one of the most frequently studied cancer-related miRNAs, predicts poor prognosis in HNSCC (10). However, in general, the overlap of prognostic miRNAs across different HNSCC studies is small. This can be potentially explained by differences in demography, treatment parameters, composition of patient subgroups (e.g., subsite and HPV status) as well as by methodological issues such as the lack of independent validation, limitations due to small sample size, the analysis of different endpoints, the number of miRNAs screened and the nonavailability of thorough clinical information including HPV status (27). Our comprehensive miRNA profiling approach deliberately and exclusively focused on HPV-negative patients based on the fact that all current data indicate a completely distinct molecular pathogenesis of HPV-associated cancer, which, meanwhile, is regarded a distinct clinical entity (2, 6).

Nevertheless, in our study we were able to confirm previously reported prognostic miRNAs in HNSCC such as hsa-miR-21-3p, hsa-let-7g-3p, hsa-miR-210-5p, and hsa-miR-210-3p (Supplementary Fig. S20), underlining the validity of our miRNA analysis (10, 22, 26, 28, 29). In addition, hsa-mir-210-5p and hsa-let-7g-3p form part of our five-miRNA signature. hsa-let-7g was shown to predict prognosis in oral cavity squamous cell

Published OnlineFirst August 31, 2018; DOI: 10.1158/1078-0432.CCR-18-0776

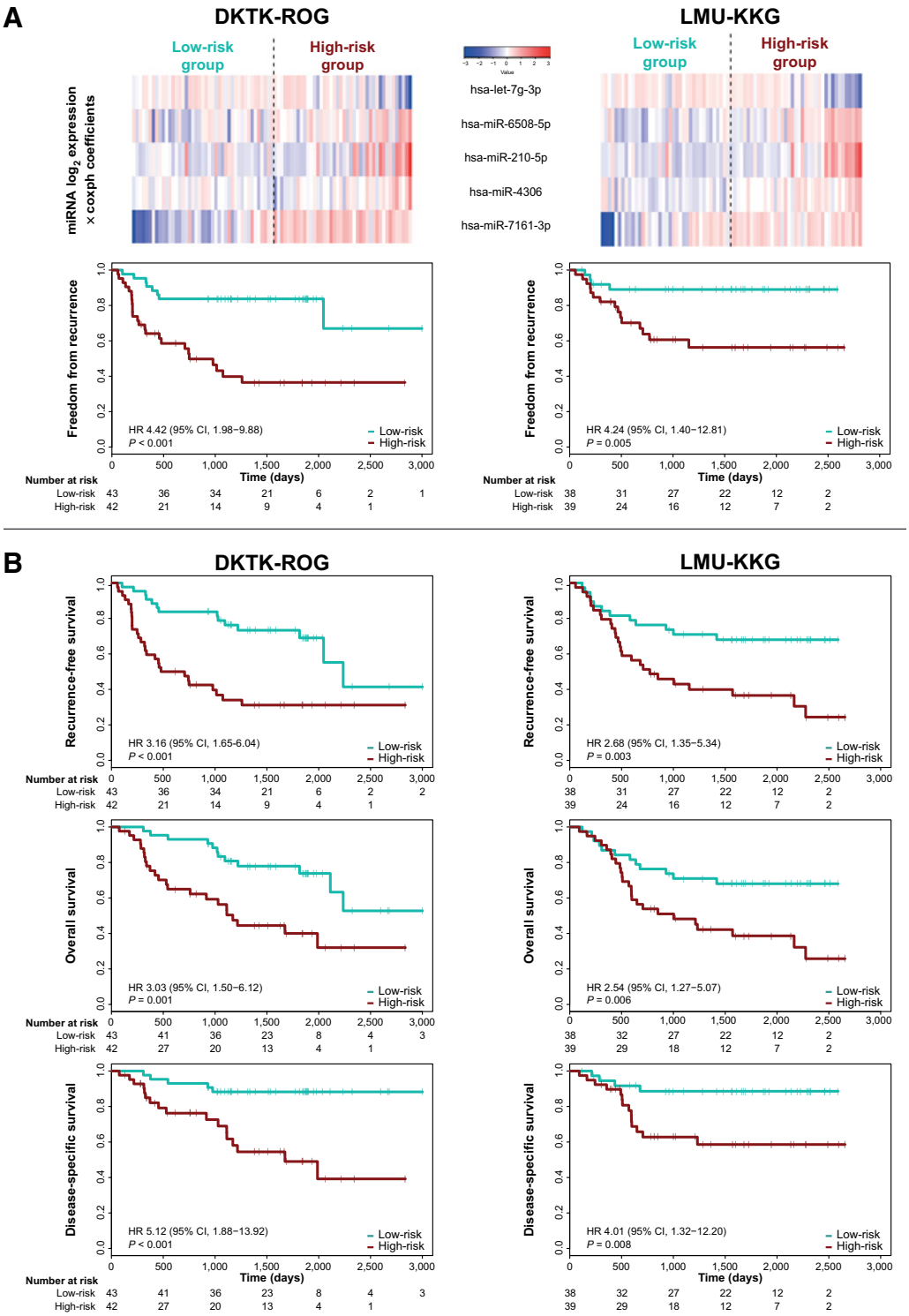

Figure 1.

Freedom from recurrence stratified by risk according to the five-miRNA signature: miRNA expression and Kaplan–Meier curves in the DKTK-ROG (training set) and the LMU-KKG (validation set) samples. **A,** Top: Heat map colors indicate scaled miRNA $\log_2$ expression values multiplied by the Cox proportional hazard coefficients (coxph) from low (blue) to high (red) on a scale from −3 to 3 for each of the five signature miRNAs in the DKTK-ROG (left) and the LMU-KKG samples (right). Bottom: Kaplan–Meier curves for the endpoint freedom from recurrence for HNSCC patients of the training set (DKTK-ROG sample; left) and the validation set (LMU-KKG sample; right) stratified into low- and high-risk patients according to the five-miRNA signature. *P* values are derived by log-rank test. **B,** Kaplan–Meier curves for recurrence-free survival (top), overall survival (middle), and disease-specific survival (bottom) in patients of the training (DKTK-ROG sample; left) and validation sets (LMU-KKG sample; right) stratified according to their risk (low- and high-risk groups) by the five-miRNA signature.

Published OnlineFirst August 31, 2018; DOI: 10.1158/1078-0432.CCR-18-0776

Table 2. Multivariate Cox regression analysis of the five-miRNA signature and clinicopathologic parameters with freedom from recurrence (training and validation sets)

	Training set DKTK-ROG		Validation set LMU-KKG	
Parameter	**HR (95% CI)**	***P* value**	**HR (95% CI)**	***P* value**
Five-miRNA signature (high-risk vs. low-risk)	5.55 (2.09–14.79)	<0.001	3.94 (1.23–12.59)	0.021
TNM T stage (T3/T4 vs. T1/T2)	2.19 (0.96–5.02)	0.064	2.71 (0.99–7.44)	0.052
LVI (yes vs. no)	2.22 (0.99–4.97)	0.053	2.50 (0.84–7.45)	0.099
ECE (yes vs. no[a])	1.45 (0.61–3.48)	0.40	2.29 (0.77–6.78)	0.13

[a]N0 tumors were included in the group of ECE-negative tumors.

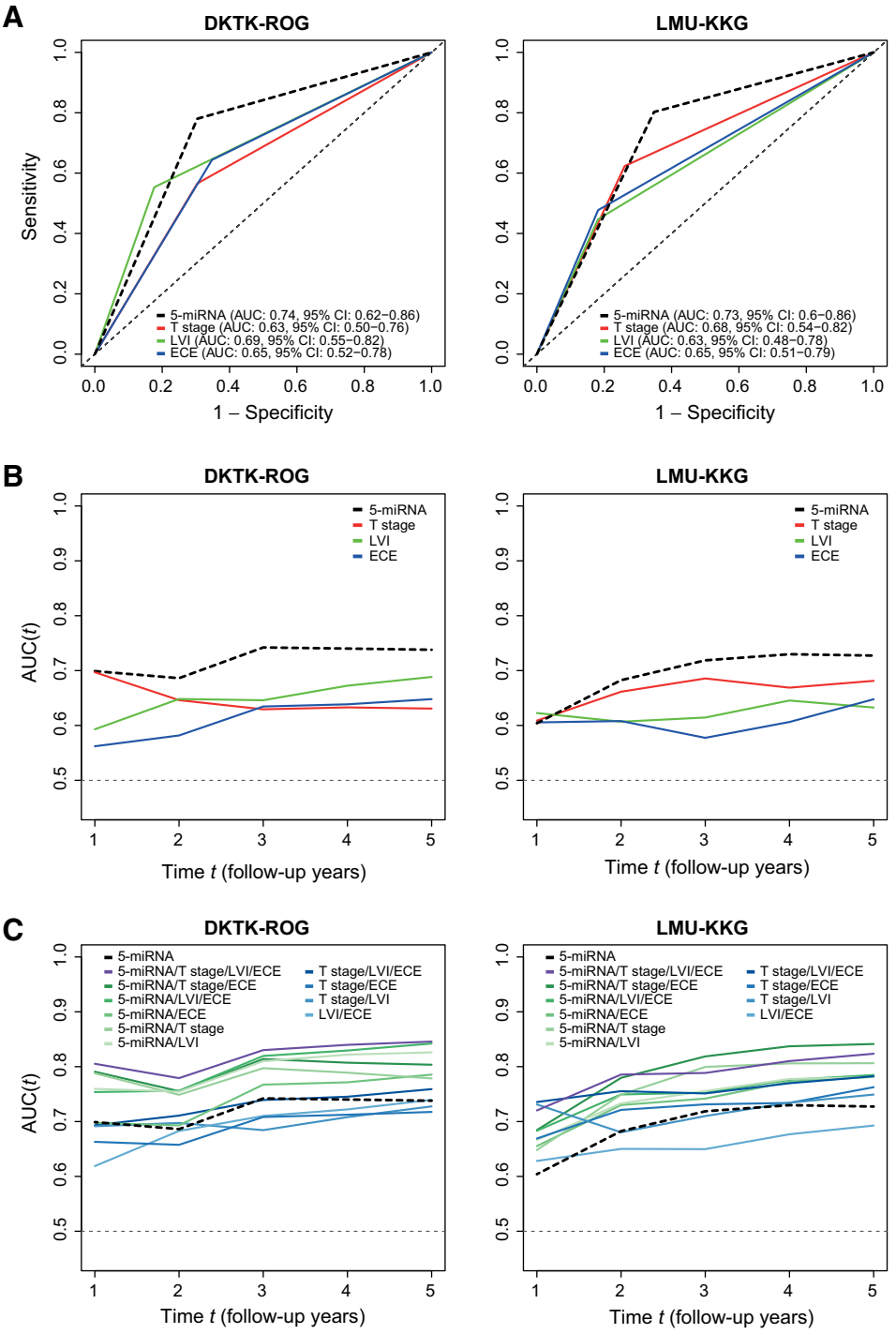

Figure 2.
Performance of the prediction of freedom from recurrence comparing the five-miRNA signature with clinicopathologic risk factors. **A,** Sensitivity- and specificity-derived AUCs for the prediction of freedom from recurrence in the DKTK-ROG (training set; left) and the LMU-KKG samples (validation set; right) at 5 follow-up years. The AUCs and the 95% CIs of the five-miRNA signature–derived risk factor (black dashed curve), TNM T stage, LVI, and ECE are shown. Time-dependent sensitivity and specificity derived AUCs for the prediction of freedom from recurrence in the DKTK-ROG (left) and the LMU-KKG samples (right) at follow-up years 1 to 5: **B,** AUCs of the five-miRNA signature–derived risk factor (black dashed curve), TNM T stage (red), LVI (green), and ECE (blue). **C,** AUCs for the five-miRNA signature–derived risk factor alone (black dashed curve); the five-miRNA signature combined with TNM T stage, LVI, and ECE (purple and greenish curves); and combinations of the clinicopathologic risk factors TNM T stage, LVI, and ECE (bluish curves).

Published OnlineFirst August 31, 2018; DOI: 10.1158/1078-0432.CCR-18-0776

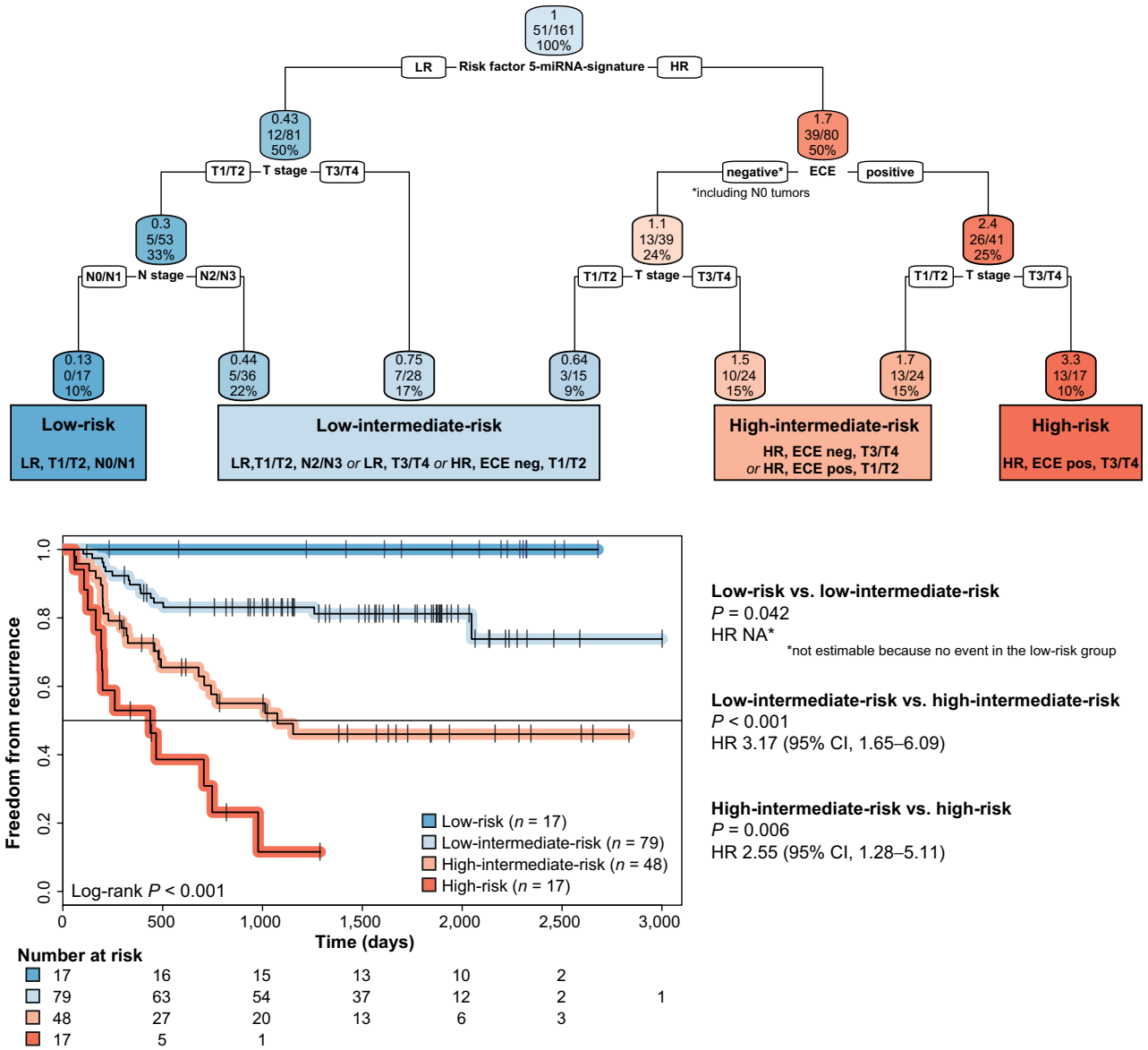

Figure 3.

Risk groups for recurrence identified by RPA. RPA tree and risk groups for recurrence combining the parameters five-miRNA signature (high-risk, low-risk), ECE (negative—including N0 tumors, positive), T stage (T1/T2, T3/T4), and N stage (N0/N1, N2/N3) in the pooled HNSCC data set ($n = 162$). Each node shows the predicted probability of recurrence (locoregional or distant failure; color code low to high: blue–red), the number of events for the total number of patients, and the percentage of observations in the node. Kaplan–Meier curves for the endpoint freedom from recurrence for the four identified risk groups "low-risk," "low-intermediate-risk," "high-intermediate-risk," and "high-risk." Multivariate and pairwise comparisons are shown. *P* values are derived by the log-rank test. See extended version Supplementary Fig. S16. neg, negative; pos, positive.

carcinoma (29) and breast cancer patients (30) via inhibition of cell invasion and metastasis. Besides head and neck cancer (28), hsa-mir-210 was already reported as prognostic factor in breast cancer (31–34), soft-tissue sarcoma (35), osteosarcoma (36), pancreatic cancer (37), non–small cell lung cancer (38), renal cancer (39), and glioblastoma (40). Multiple functions of hsa-miR-210 are described including hypoxic response, regulation of mitochondrial metabolism, cell cycle, cell survival, differentiation, DNA repair, and immune response (41). To the best of our knowledge, the remaining three signature miRNAs (hsa-miR-6508-5p, hsa-miR-4306, and hsa-miR-7161-3p) have not yet been associated with HNSCC or cancer in general.

miRNAs are integrative regulator molecules with a highly promiscuous nature, thereby interfering with multiple pathways. Thus, it is not possible to deduce a definitive functional role of a given miRNA within a signaling network. Nevertheless, studying the miRNA–mRNA target network, our five-miRNA signature suggests enrichment of specific signaling pathways: *p53*, *ATM*, *FoxO* signaling, and DNA double-strand break response, pre-NOTCH expression and processing, as well as

mitosis and senescence-associated pathways. Several of the pathways and miRNA-target genes were already shown to be relevant for the pathogenesis and radiation response of HNSCC (5–7, 42–47). Mutations of *IGF1R* and *ARID1A* and the involvement of CADM1 and SOD2 in HNSCC have been reported (6, 43, 46, 47).

Gene expression relates to prognosis of HNSCC (48) as does a seven-gene signature, recently also described in our patients (49); this signature, however, predicts freedom from recurrence independently from the above-mentioned five-miRNA signature (unpublished). Analogous to their prognostic independence the molecular impact of the Schmidt and colleagues seven-gene signature shows no obvious overlap with that of our five-miRNA signature (49). However, to pin down mechanisms and pathogenic relevance of the five-miRNA signature, further studies are required.

At present, treatment decisions for patients with HNSCC are guided predominantly by clinical findings. The only relevant biological marker with yet limited influence on treatment decisions is HPV status (1). A key prerequisite for the potential clinical application of a molecular signature is a robust, fast, and easy to perform laboratory assay. Our qRT-PCR validation of the high-throughput omics data is a first step in this direction.

The five-miRNA signature's potential is particularly exemplified by the fact that, when combined with the clinically relevant prognostic parameters TNM T stage, ECE, and TNM N stage, it allowed the significant stratification of patients into four risk groups for recurrence. Strikingly, in this context, the five-miRNA signature was the strongest factor for patient stratification. Furthermore, the integration of the molecular signature with clinical factors not only improved the prediction of outcome but also allowed a more detailed, clinically meaningful stratification of patients, which, in turn, could be used as a clinical patient stratification tool.

Possible personalized treatment options include consideration of adjusting therapy intensity according to the overall risk for therapy failure. In particular, patients with the highest risk of recurrence, for whom the standard treatment is not sufficient, might be candidates for more personalized treatment options such as the addition of targeted drugs or immune-checkpoint inhibitors to radio(chemo)therapy, dose escalation or further (neo)adjuvant chemotherapy. On the other hand, for patients with the lowest risk of recurrence de-escalation strategies for the reduction of therapy-associated toxicity could be considered. Here, dose de-escalation and the omission of chemotherapy would be options, as the long-term benefit from the addition of simultaneous chemotherapy to radiotherapy is not given for all patients (50). Further, the five-miRNA signature represents the basis for a more focused search for molecular therapeutic targets improving therapy success for appropriate patients.

In order to evaluate the predictive value of the five-miRNA signature for the guidance of treatment decisions, prospective validation studies and clinical trials considering treatment stratification are required in the future.

In summary, the herein identified prognostic five-miRNA signature independently predicts disease control and survival of HPV-negative patients. The target gene network of the signature miRNAs is well in line with known mechanisms driving HNSCC pathogenesis. In combination with established prognostic clinical parameters, the ability of the signature to predict disease control and survival even improves and allows the definition of four prognostically distinct groups. These may provide an important step toward personalized HNSCC treatment.

Disclosure of Potential Conflicts of Interest

T. Kirchner reports receiving other commercial research support from Merck and Roche, reports receiving speakers bureau honoraria from Merck and AstraZeneca, and is a consultant/advisory board member for Amgen, AstraZeneca, Bristol-Myers Squibb, Merck KGaA, MSD Sharp & Dohme, Novartis, Pfizer, Roche Pharma Research Funding, Merck, and Roche. J. Debus reports receiving commercial research grants from Merck Serono. C. Belka reports receiving other commercial research support from Merck Darmstadt and Elekta, reports receiving speakers bureau honoraria from Merck Darmstadt, and is a consultant/advisory board member for Merck Darmstadt, Bristol-Myers Squibb, and AstraZeneca. No potential conflicts of interest were disclosed by the other authors.

Authors' Contributions

Conception and design: J. Hess, K. Unger, C. Maihoefer, J. Debus, A.-L. Grosu, M. Stuschke, D. Zips, H. Zitzelsberger, M. Henke, C. Belka

Development of methodology: K. Unger, L. Wintergerst, M. Werner

Acquisition of data (provided animals, acquired and managed patients, provided facilities, etc.): J. Hess, C. Maihoefer, L. Schüttrumpf, L. Wintergerst, S. Marschner, S. Kuger, U. Pflugradt, P. Baumeister, A. Walch, C. Woischke, T. Kirchner, M. Werner, M. Baumann, S.E. Combs, J. Debus, A.-L. Grosu, A. Linge, C. Rödel, M. Stuschke, U. Ganswindt, M. Henke, C. Belka

Analysis and interpretation of data (e.g., statistical analysis, biostatistics, computational analysis): J. Hess, K. Unger, C. Maihoefer, H. Braselmann, D. Samaga, A. Walch, C. Woischke, T. Kirchner, K. Werner, M. Baumann, D. Zips, U. Ganswindt, M. Henke, C. Belka

Writing, review, and/or revision of the manuscript: J. Hess, K. Unger, C. Maihoefer, L. Schüttrumpf, L. Wintergerst, T. Heider, P. Weber, S. Marschner, H. Braselmann, D. Samaga, M. Werner, M. Baumann, V. Budach, S.E. Combs, J. Debus, M. Krause, A. Linge, C. Rödel, M. Stuschke, D. Zips, H. Zitzelsberger, U. Ganswindt, M. Henke, C. Belka

Administrative, technical, or material support (i.e., reporting or organizing data, constructing databases): J. Hess, C. Maihoefer, T. Heider, P. Weber, S. Marschner, U. Pflugradt, T. Kirchner, J. Debus, A.-L. Grosu, M. Stuschke, U. Ganswindt, M. Henke

Study supervision: J. Hess, U. Pflugradt, H. Zitzelsberger, U. Ganswindt, M. Henke, C. Belka

Other (coordination of the multi-center study consortium): M. Krause

Acknowledgments

This study was supported by the DKTK-ROG and the Clinical Cooperation Group "Personalized Radiotherapy in Head and Neck Cancer," Helmholtz Zentrum München.

The authors want to thank L. Dajka, S. Heuer, C. Innerlohinger, U Buchholz, and C.-M. Pflüger for their excellent technical assistance; R. Caldwell for editorial assistance; all coworkers of the Clinical Cooperation Group "Personalized Radiotherapy in Head and Neck Cancer" for scientific support; and all members of the DKTK-ROG for their valuable contribution to the DKTK-ROG data set.

This study was supported by the German Federal Ministry of Education and Research project ZiSStrans (02NUK047A, 02NUK047C, and 02NUK047F) and the Joint Funding Grant within the German Consortium for Translational Cancer Research (DKTK) awarded to the DKTK-ROG (Radiation Oncology Group). The DKTK is funded as one of the National German Health Centers by the German Federal Ministry of Education and Research.

The costs of publication of this article were defrayed in part by the payment of page charges. This article must therefore be hereby marked *advertisement* in accordance with 18 U.S.C. Section 1734 solely to indicate this fact.

Received March 20, 2018; revised July 19, 2018; accepted August 27, 2018; published first August 31, 2018.

Published OnlineFirst August 31, 2018; DOI: 10.1158/1078-0432.CCR-18-0776

References

1. O'Sullivan B, Huang SH, Siu LL, Waldron J, Zhao H, Perez-Ordonez B, et al. Deintensification candidate subgroups in human papillomavirus-related oropharyngeal cancer according to minimal risk of distant metastasis. J Clin Oncol 2013;31:543–50.
2. O'Sullivan B, Huang SH, Su J, Garden AS, Sturgis EM, Dahlstrom K, et al. Development and validation of a staging system for HPV-related oropharyngeal cancer by the International Collaboration on Oropharyngeal cancer Network for Staging (ICON-S): a multicentre cohort study. Lancet Oncol 2016;17:440–51.
3. Bossi P, Alfieri S. Investigational drugs for head and neck cancer. Expert Opin Investig Drugs 2016;25:797–810.
4. Argiris A, Harrington KJ, Tahara M, Schulten J, Chomette P, Ferreira Castro A, et al. Evidence-based treatment options in recurrent and/or metastatic squamous cell carcinoma of the head and neck. Front Oncol 2017;7:72.
5. Agrawal N, Frederick MJ, Pickering CR, Bettegowda C, Chang K, Li RJ, et al. Exome sequencing of head and neck squamous cell carcinoma reveals inactivating mutations in NOTCH1. Science 2011;333:1154–7.
6. Cancer Genome Atlas N. Comprehensive genomic characterization of head and neck squamous cell carcinomas. Nature 2015;517:576–82.
7. Stransky N, Egloff AM, Tward AD, Kostic AD, Cibulskis K, Sivachenko A, et al. The mutational landscape of head and neck squamous cell carcinoma. Science 2011;333:1157–60.
8. Bagnoli M, Canevari S, Califano D, Losito S, Maio MD, Raspagliesi F, et al. Development and validation of a microRNA-based signature (MiROvaR) to predict early relapse or progression of epithelial ovarian cancer: a cohort study. Lancet Oncol 2016;17:1137–46.
9. Iorio MV, Croce CM. MicroRNA dysregulation in cancer: diagnostics, monitoring and therapeutics. A comprehensive review. EMBO Mol Med 2012;4:143–59.
10. Jamali Z, Asl Aminabadi N, Attaran R, Pournagiazar F, Ghertasi Oskouei S, Ahmadpour F. MicroRNAs as prognostic molecular signatures in human head and neck squamous cell carcinoma: a systematic review and meta-analysis. Oral Oncol 2015;51:321–31.
11. Koshizuka K, Hanazawa T, Fukumoto I, Kikkawa N, Okamoto Y, Seki N. The microRNA signatures: aberrantly expressed microRNAs in head and neck squamous cell carcinoma. J Hum Genet 2017;62:3–13.
12. Sethi N, Wright A, Wood H, Rabbitts P. MicroRNAs and head and neck cancer: reviewing the first decade of research. Eur J Cancer 2014;50:2619–35.
13. Lohaus F, Linge A, Tinhofer I, Budach V, Gkika E, Stuschke M, et al. HPV16 DNA status is a strong prognosticator of loco-regional control after postoperative radiochemotherapy of locally advanced oropharyngeal carcinoma: results from a multicentre explorative study of the German Cancer Consortium Radiation Oncology Group (DKTK-ROG). Radiother Oncol 2014;113:317–23.
14. Maihoefer C, Schüttrumpf L, Macht C, Pflugradt U, Hess J, Schneider L, et al. Postoperative (chemo) radiation in patients with squamous cell cancers of the head and neck – clinical results from the cohort of the clinical cooperation group "Personalized Radiotherapy in Head and Neck Cancer". Radiation Oncology 2018;13:123.
15. R Core Team. R: A Language and Environment for Statistical Computing. R Foundation for Statistical Computing; 2016.
16. Cho H, Yu A, Kim S, Kang J, Hong S-M. Robust likelihood-based survival modeling with microarray data. J Stat Soft 2009;29:16.
17. Niyazi M, Pitea A, Mittelbronn M, Steinbach J, Sticht C, Zehentmayr F, et al. A 4-miRNA signature predicts the therapeutic outcome of glioblastoma. Oncotarget 2016;7:45764–75.
18. Fabregat A, Sidiropoulos K, Garapati P, Gillespie M, Hausmann K, Haw R, et al. The Reactome pathway Knowledgebase. Nucleic Acids Res 2016;44:D481–7.
19. Piccirillo JF, Vlahiotis A. Comorbidity in patients with cancer of the head and neck: prevalence and impact on treatment and prognosis. Curr Oncol Rep 2006;8:123–9.
20. Zhang JX, Song W, Chen ZH, Wei JH, Liao YJ, Lei J, et al. Prognostic and predictive value of a microRNA signature in stage II colon cancer: a microRNA expression analysis. Lancet Oncol 2013;14:1295–306.
21. Liu N, Chen NY, Cui RX, Li WF, Li Y, Wei RR, et al. Prognostic value of a microRNA signature in nasopharyngeal carcinoma: a microRNA expression analysis. Lancet Oncol 2012;13:633–41.
22. Ganci F, Sacconi A, Manciocco V, Sperduti I, Battaglia P, Covello R, et al. MicroRNA expression as predictor of local recurrence risk in oral squamous cell carcinoma. Head Neck 2016;38:E189–97.
23. Gao G, Gay HA, Chernock RD, Zhang TR, Luo J, Thorstad WL, et al. A microRNA expression signature for the prognosis of oropharyngeal squamous cell carcinoma. Cancer 2013;119:72–80.
24. Hess AK, Muer A, Mairinger FD, Weichert W, Stenzinger A, Hummel M, et al. MiR-200b and miR-155 as predictive biomarkers for the efficacy of chemoradiation in locally advanced head and neck squamous cell carcinoma. Eur J Cancer 2017;77:3–12.
25. Shi H, Chen J, Li Y, Li G, Zhong R, Du D, et al. Identification of a six microRNA signature as a novel potential prognostic biomarker in patients with head and neck squamous cell carcinoma. Oncotarget 2016;7:21579–90.
26. Wong N, Khwaja SS, Baker CM, Gay HA, Thorstad WL, Daly MD, et al. Prognostic microRNA signatures derived from The Cancer Genome Atlas for head and neck squamous cell carcinomas. Cancer Med 2016;5:1619–28.
27. Shi X, Yi H, Ma S. Measures for the degree of overlap of gene signatures and applications to TCGA. Brief Bioinform 2015;16:735–44.
28. Gee HE, Camps C, Buffa FM, Patiar S, Winter SC, Betts G, et al. hsa-mir-210 is a marker of tumor hypoxia and a prognostic factor in head and neck cancer. Cancer 2010;116:2148–58.
29. Peng SC, Liao CT, Peng CH, Cheng AJ, Chen SJ, Huang CG, et al. MicroRNAs MiR-218, MiR-125b, and Let-7g predict prognosis in patients with oral cavity squamous cell carcinoma. PLoS One 2014;9:e102403.
30. Qian P, Zuo Z, Wu Z, Meng X, Li G, Wu Z, et al. Pivotal role of reduced let-7g expression in breast cancer invasion and metastasis. Cancer Res 2011;71:6463–74.
31. Camps C, Buffa FM, Colella S, Moore J, Sotiriou C, Sheldon H, et al. hsa-miR-210 Is induced by hypoxia and is an independent prognostic factor in breast cancer. Clin Cancer Res 2008;14:1340–8.
32. Rothe F, Ignatiadis M, Chaboteaux C, Haibe-Kains B, Kheddoumi N, Majjaj S, et al. Global microRNA expression profiling identifies MiR-210 associated with tumor proliferation, invasion and poor clinical outcome in breast cancer. PLoS One 2011;6:e20980.
33. Volinia S, Galasso M, Sana ME, Wise TF, Palatini J, Huebner K, et al. Breast cancer signatures for invasiveness and prognosis defined by deep sequencing of microRNA. Proc Natl Acad Sci U S A 2012;109:3024–9.
34. Buffa FM, Camps C, Winchester L, Snell CE, Gee HE, Sheldon H, et al. microRNA-associated progression pathways and potential therapeutic targets identified by integrated mRNA and microRNA expression profiling in breast cancer. Cancer Res 2011;71:5635–45.
35. Greither T, Wurl P, Grochola L, Bond G, Bache M, Kappler M, et al. Expression of microRNA 210 associates with poor survival and age of tumor onset of soft-tissue sarcoma patients. Int J Cancer 2012;130:1230–5.
36. Cai H, Lin L, Cai H, Tang M, Wang Z. Prognostic evaluation of microRNA-210 expression in pediatric osteosarcoma. Med Oncol 2013;30:499.
37. Greither T, Grochola LF, Udelnow A, Lautenschlager C, Wurl P, Taubert H. Elevated expression of microRNAs 155, 203, 210 and 222 in pancreatic tumors is associated with poorer survival. Int J Cancer 2010;126:73–80.
38. Eilertsen M, Andersen S, Al-Saad S, Richardsen E, Stenvold H, Hald SM, et al. Positive prognostic impact of miR-210 in non-small cell lung cancer. Lung Cancer 2014;83:272–8.
39. McCormick RI, Blick C, Ragoussis J, Schoedel J, Mole DR, Young AC, et al. miR-210 is a target of hypoxia-inducible factors 1 and 2 in renal cancer, regulates ISCU and correlates with good prognosis. Br J Cancer 2013;108:1133–42.
40. Qiu S, Lin S, Hu D, Feng Y, Tan Y, Peng Y. Interactions of miR-323/miR-326/miR-329 and miR-130a/miR-155/miR-210 as prognostic indicators for clinical outcome of glioblastoma patients. J Transl Med 2013;11:10.
41. Qin Q, Furong W, Baosheng L. Multiple functions of hypoxia-regulated miR-210 in cancer. J Exp Clin Cancer Res 2014;33:50.
42. Hess J, Unger K, Orth M, Schotz U, Schuttrumpf L, Zangen V, et al. Genomic amplification of Fanconi anemia complementation group A (FancA) in head and neck squamous cell carcinoma (HNSCC): Cellular mechanisms of radioresistance and clinical relevance. Cancer Lett 2017;386:87–99.
43. Lui VW, Hedberg ML, Li H, Vangara BS, Pendleton K, Zeng Y, et al. Frequent mutation of the PI3K pathway in head and neck cancer defines predictive biomarkers. Cancer Discov 2013;3:761–9.

Published OnlineFirst August 31, 2018; DOI: 10.1158/1078-0432.CCR-18-0776

44. Michna A, Schotz U, Selmansberger M, Zitzelsberger H, Lauber K, Unger K, et al. Transcriptomic analyses of the radiation response in head and neck squamous cell carcinoma subclones with different radiation sensitivity: time-course gene expression profiles and gene association networks. Radiat Oncol 2016;11:94.
45. Summerer I, Hess J, Pitea A, Unger K, Hieber L, Selmansberger M, et al. Integrative analysis of the microRNA–mRNA response to radiochemotherapy in primary head and neck squamous cell carcinoma cells. BMC Genomics 2015;16:654.
46. Vallath S, Sage EK, Kolluri KK, Lourenco SN, Teixeira VS, Chimalapati S, et al. CADM1 inhibits squamous cell carcinoma progression by reducing STAT3 activity. Sci Rep 2016;6:24006.
47. Ye H, Wang A, Lee BS, Yu T, Sheng S, Peng T, et al. Proteomic based identification of manganese superoxide dismutase 2 (SOD2) as a metastasis marker for oral squamous cell carcinoma. Cancer Genomics Proteomics 2008;5:85–94.
48. Tonella L, Giannoccaro M, Alfieri S, Canevari S, De Cecco L. Gene expression signatures for head and neck cancer patient stratification: are results ready for clinical application? Curr Treat Options Oncol 2017;18:32.
49. Schmidt S, Linge A, Zwanenburg A, Leger S, Lohaus F, Krenn C, et al. Development and validation of a gene signature for patients with head and neck carcinomas treated by postoperative radio(chemo)therapy. Clin Cancer Res 2018;24:1364–74.
50. Cooper JS, Zhang Q, Pajak TF, Forastiere AA, Jacobs J, Saxman SB, et al. Long-term follow-up of the RTOG 9501/intergroup phase III trial: postoperative concurrent radiation therapy and chemotherapy in high-risk squamous cell carcinoma of the head and neck. Int J Radiat Oncol Biol Phys 2012;84:1198–205.

Published OnlineFirst August 31, 2018; DOI: 10.1158/1078-0432.CCR-18-0776

AACR American Association for Cancer Research

Clinical Cancer Research

A Five-MicroRNA Signature Predicts Survival and Disease Control of Patients with Head and Neck Cancer Negative for HPV Infection

Julia Hess, Kristian Unger, Cornelius Maihoefer, et al.

Clin Cancer Res Published OnlineFirst August 31, 2018.